Current Applied Physics 11 (2011) S293–S296

Contents lists available at ScienceDirect

Current Applied Physics

journal homepage: www.elsevier.com/locate/cap

Influence of exchange-correlation functionals on dielectric properties of rutile TiO_2

Bora Lee [a], Choong-ki Lee [b], Cheol Seong Hwang [a], Seungwu Han [a,*]

[a] Department of Materials Science and Engineering, Seoul National University, Seoul 151-744, Republic of Korea
[b] School of Physics, Korea Institute for Advanced Study, Seoul 130-722, Republic of Korea

ARTICLE INFO

Article history:
Received 31 August 2010
Received in revised form
23 November 2010
Accepted 26 November 2010
Available online 4 December 2010

Keywords:
Dielectric constant
Hybrid functional
LDA + *U*
TiO_2
Phonon mode

ABSTRACT

We investigate dielectric properties of rutile TiO_2 using various exchange-correlation energy functionals such as local-density approximation (LDA), LDA + *U* method, and hybrid functionals. It is found that the computed dielectric constants significantly depend on the functional type, which originates from hardening or softening of phonon modes. While LDA provides the best result among the tested functionals, hybrid functionals and LDA + *U* methods significantly overestimate and underestimate dielectric constants, respectively. The underestimation by LDA + *U* is most alarming as it is not alleviated by adjusting lattice parameters, which implies that interatomic interactions are fundamentally affected by LDA + *U*. Furthermore, the LDA + *U* method also underestimates the dielectric constant of cubic $SrTiO_3$. The present results suggest that special cares are needed in applying the LDA + *U* method to a system including TiO_2 and $SrTiO_3$.

1. Introduction

Rutile TiO_2 is a versatile functional oxide that comprises crucial components in various devices used in information and energy technologies. The catalytic effects of TiO_2 surfaces have attracted a great deal of interest toward energy conversion and hydrogen production. TiO_2 is also a strong candidate material to be used as insulating parts in highly scaled electronic devices [1]. In every application, the high static dielectric constant (ε^0) of TiO_2, 111 and 257 along *a* and *c* axes, respectively [2], is an essential material property that underlies the outstanding device performance.

The unique dielectric properties of TiO_2 are related to its soft phonon modes. In Ref. [3], the lattice-dynamical dielectric response of rutile was investigated in detail with the density functional perturbation theory based on the local-density approximation (LDA), and excellent agreements with experiment were found. When the generalized gradient approximation (GGA) is applied, the ferroelectric instability was found [4]. However, the semilocal functionals such as LDA or GGA have critical drawbacks, particularly when applied to titanates. First, it is well known that the energy gap computed with semilocal functionals is always underestimated by 30–40%. The band-gap problem is particularly acute in TiO_2 or $SrTiO_3$ with an energy gap of ~3 eV since various defect and interfacial properties can be qualitatively influenced by the gap reduction. Second, due to the correlated nature of Ti 3*d* electrons, the electronic structure of titanates with substantial Ti 3*d* occupation is not properly described by semilocal functionals. A well-known example is the semiconducting property of $LaTiO_3$ [5]. To overcome these fundamental limits in semilocal functionals, other approaches such as LDA + *U* methods or hybrid functionals have been actively employed with noteworthy successes [5–10].

In spite of recent trends in employing LDA + *U* or hybrid functional methods to study complex properties of titanates, it has not been carefully examined whether these advanced methods provide correct dielectric properties. We address this basic issue in this paper by calculating the dielectric property of rutile TiO_2 with various energy functionals such as LDA, LDA + *U*, and hybrid functionals. Our results demonstrate that interatomic interactions significantly depend on the exchange-correlation functional and special cares are called for in using methods beyond semilocal functionals on TiO_2.

2. Computational methods

We carry out first-principles calculations using the computational code of Vienna *Ab initio* Simulation Package (VASP) [11]. The conventional density-functional calculations are carried out using

* Corresponding author.
E-mail address: hansw@snu.ac.kr (S. Han).

1567-1739/$ – see front matter © 2010 Elsevier B.V. All rights reserved.
doi:10.1016/j.cap.2010.11.104

LDA [12], GGA [13], and LDA + U methods [14]. Among various hybrid functional schemes, PBE0 [15] and HSE06 [16] functionals are employed as they are found to be suitable for solid-state materials. The ionic potentials are described by the projector-augmented wave (PAW) pseudopotential [17], and the valence configurations of $3s^2 3p^6 4s^2 3d^2$ and $2s^2 2p^4$ are used for Ti and O atoms, respectively. The energy cutoff to describe electronic wave functions is chosen to be 500 eV. The k points on a $4 \times 4 \times 6$ regular mesh are sampled for the Brillouin-zone integration except for the finite field calculations (see below) where the k points are sampled on a finer mesh of $6 \times 6 \times 8$. For LDA + U methods applied on Ti $3d$ orbitals, we select two sets of Coulomb (U) and exchange (J) parameters in the model Hamiltonian: ($U = 3.2$ eV, $J = 0.9$ eV) or ($U = 5.0$ eV, $J = 0.64$ eV) [8]. In Ref. [6], a self-consistent Coulomb parameter was found to be 3.4 eV for rutile TiO_2 and therefore, the first set would be a more sound choice. As we employ the rotationally invariant form suggested in Ref. [14], the model Hamiltonian depends only on $U - J$ ($=U_{\text{eff}}$). For each method, the atomic positions and lattice parameters are relaxed independently until the atomic forces and stress tensors are reduced below 0.01 eV/Å and 10 kbar, respectively.

To compute Born effective charges, zone-center phonon frequencies, and dielectric constants (optical and static), a linear-response theory [18] implemented in VASP is used. For the hybrid functionals, however, the present version of VASP does not support the linear-response approach and therefore, we calculate the phonon frequency by diagonalizing the Hessian matrix obtained by the finite-difference method. In addition, Born effective charges and optical dielectric constants are calculated by applying finite electric fields. We confirm the consistency of the two approaches (that is to say, full linear-response approach versus finite difference plus finite field methods) by carrying out calculations within LDA. It is found that Born effective charges and optical dielectric constants differ by less than 0.5% between the two methods. The phonon frequencies agree within 2% (maximum errors for A_{2u} and E_u modes) which results in 6% discrepancy in static dielectric constants. This level of agreement is enough for the following discussions.

3. Results and discussions

First, we calculate the equilibrium lattice parameters of rutile TiO_2 as summarized in Table 1. Overall, every method reproduces the experimental values within 2% but the results based on the hybrid functional method are in best agreement with experiment. In general, the overestimated lattice parameters in GGA calculations are reduced by addition of exact exchange interactions [19]. We also calculate the energy gap of TiO_2 in Table 1. (TiO_2 has a direct band gap at the Γ point.) It is found that the HSE06 result of 3.39 eV is closest to the experimental value of 3.00 eV [20]. In Ref. [7], the band gap of TiO_2 was fitted to the experimental value by reducing the relative weight of the Hartree-Fock exchange energy in HSE06 from 0.25 to 0.2.

The computed optical dielectric constants (ε_a^∞ and ε_c^∞ along a and c axis, respectively) are presented in fourth and fifth rows in Table 1. It is seen that ε^∞ decreases monotonically with the energy gap but the gap dependence is much weaker in hybrid functionals. Even though the HSE06 predicts an energy gap closest to experiment, ε^∞ is significantly reduced. On the other hand, ε^∞ from the LDA + U method with smaller U_{eff} agrees well with experimental values. It is noted that ε^∞ from the LDA method is in good agreement with a previous calculation ($\varepsilon_a^\infty = 6.37$ and $\varepsilon_c^\infty = 7.29$) [3]. The last two rows in Table 1 display the static dielectric constants of TiO_2 (ε_a and ε_c). As GGA functionals give rise to an imaginary component in the phonon spectrum [4], the method is not considered in evaluating ε^0. Since the present theoretical calculation is based on the zero-temperature formalism, we compare computational results to the experimental data at low temperature (1.6 K) [2]. It is found that the LDA results match best with experimental data among the tested functionals. The present LDA values are larger than previous results in Ref. [3] by 20% ($\varepsilon_a = 117.5$ and $\varepsilon_c = 165.4$). This is caused by the difference in soft phonon modes which are highly sensitive to lattice parameters (see below). In Table 1, results from other functionals are not satisfactory. For instance, the hybrid functional methods overestimate the dielectric constant by ~150%. In contrast, the LDA + U approach yields dielectric constants far smaller than the reference values, particularly for ε_c which is reduced by a factor of 4–5. It is also noted that a larger U_{eff} exacerbates the underestimation. Therefore, if one increases U_{eff} to expand the energy gap, the error in the dielectric constant becomes more serious. For comparison, we also tested GGA + U functionals but the computed dielectric constants are similar to the LDA + U results. (The lattice parameters by GGA + U are smaller than the GGA values, which results in the stable rutile structure.)

Since the electronic contribution to static dielectric constants is less than 10, the large variations among different energy functionals should originate from the lattice component of the static dielectric constant. This in turn depends on the Born effective charges and zone-center phonon frequencies. In order to identify the microscopic origin, we first examine the Born effective charges in Table 2. The Born effective charges calculated with LDA, GGA, and PBE0 methods in Ref. [21] agree with the present results within 2%. It is found that the effective charges do not vary much between different energy functionals (less than 10%) and therefore cannot account for the large variations in ε^0.

Next, we compare the phonon frequencies at the zone center. Among the various phonon modes, the lowest IR-active A_{2u} and E_u modes contribute most to ε_a and ε_c, respectively, each making up 27.9 and 13.7% of dielectric constants. These two modes are pictorially described in Fig. 1(a) and their frequencies are presented in Fig. 1(b). The vibrational frequencies of A_{2u} and E_u modes by the LDA method agree with previous calculations within 20% [3,4], which leads to the disagreement in static dielectric constants (see above). This is a result of slightly different lattice parameters which in turn are caused by different types of pseudopotentials. In Fig. 1(b), the solid line indicates the experimental frequency of the E_u mode at 300 K [22] and the dashed lines show those for the A_{2u} mode at 4 K

Table 1
Lattice parameters (a and c), band gap (E_g), and optical (ε_a^∞ and ε_c^∞) and static (ε_a and ε_c) dielectric constants of TiO_2.

	LDA	GGA	LDA + U ($U_{\text{eff}} = 2.3$ eV)	LDA + U ($U_{\text{eff}} = 4.36$ eV)	PBE0	HSE06	Exp.
a (Å)	4.558	4.650	4.575	4.585	4.587	4.588	4.587 [27]
c (Å)	2.926	2.972	2.953	2.980	2.951	2.951	2.954 [27]
E_g (eV)	1.81	1.80	2.06	2.30	4.14	3.39	3.0 [20]
ε_a^∞	7.69	7.55	6.99	6.44	5.70	5.74	6.84 [22]
ε_c^∞	8.91	9.02	8.09	7.44	6.74	6.77	8.43 [22]
ε_a	149.6	–	58.9	37.7	241.3	277.5	111 [2]
ε_c	230.6	–	73.3	44.6	363.7	401.7	257 [2]

Table 2
Born effective charge tensors of TiO_2 calculated with various functionals. The sign of off-diagonal components vary over atom sites.

	Ti			O		
	$Z^*_{xx(yy)}$	$Z^*_{xy(yx)}$	Z^*_{zz}	$Z^*_{xx(yy)}$	$Z^*_{xy(yx)}$	Z^*_{zz}
LDA	6.37	±1.02	7.64	−3.20	±1.83	−3.83
GGA	6.30	±1.04	7.76	−3.15	±1.81	−3.89
LDA + U (U_{eff} = 2.3 eV)	6.05	±0.95	7.20	−3.03	±1.69	−3.61
LDA + U (U_{eff} = 4.36 eV)	5.77	±0.89	6.85	−2.89	±1.57	−3.43
PBE0	5.98	±0.89	7.33	−2.99	±1.66	−3.62
HSE06	5.88	±0.89	7.26	−2.98	±1.65	−3.61

Table 3
The dielectric constant of TiO_2 calculated with various lattice parameters. l_0 indicates the equilibrium lattice parameters determined within each functional. l_{LDA} and l_{exp} are lattice parameters from the LDA calculation and experiment, respectively. U_{eff} of 2.3 eV is used for the LDA + U method.

	ε_a			ε_c		
	l_0	l_{LDA}	$l_{exp.}$	l_0	l_{LDA}	$l_{exp.}$
LDA	149.6	149.6	292.7	230.6	230.6	813.7
LDA + U	58.9	52.7	61.8	73.3	61.0	75.5
PBE0	216.40	111.20	224.24	322.48	170.58	345.66
HSE06	244.98	119.38	294.53	350.62	182.41	346.87

[23] and 300 K [22]. It can be seen that the functional dependence of the phonon mode is well correlated with ε^0 in Table 1. For example, the hardening of phonon mode in the LDA + U methods explains the large reduction of dielectric constants. Furthermore, the hardening of the A_{2u} mode is more pronounced than for the E_u mode, which is consistent with the above result that ε_c is suppressed more severely than ε_a. In contrast, slight softening is noticed for PBE0 or HSE06. Other phonon modes also behave in similar ways, i.e., they are hardened in LDA + U calculations and softened in the hybrid functional calculations.

It is well known that the dielectric response of TiO_2 is sensitive to the strain. This poses a question whether the underestimation or overestimation of ε^0 in LDA + U or hybrid functional methods is related to the different equilibrium lattice parameters. To this end, we compute in Table 3 the dielectric constants of TiO_2 with the lattice parameters adjusted to LDA values or experimental data. It is noticeable that ε_a and ε_c change monotonically with respect to the lattice parameters, i.e., compressive (tensile) stress reduces (increases) the dielectric constants. In particular, the dielectric constants calculated with the hybrid functionals are in good agreement with experiment (and LDA results) when the lattice parameters are reduced to LDA values. In the case of LDA calculations, increasing the lattice parameters to the experimental values significantly increases ε^0. These results indicate that the lattice parameter, rather than the exchange-correlation functional, is a decisive factor in the dielectric response within LDA and hybrid methods. A similar observation was noted for $SrTiO_3$ and $BaTiO_3$ [24]. However, ε_a and ε_c in the LDA + U method are much less sensitive to the strain and they do not approach the experimental value unless the lattice constants are expanded unrealistically. This means that interatomic interactions are significantly altered when the LDA + U method is applied.

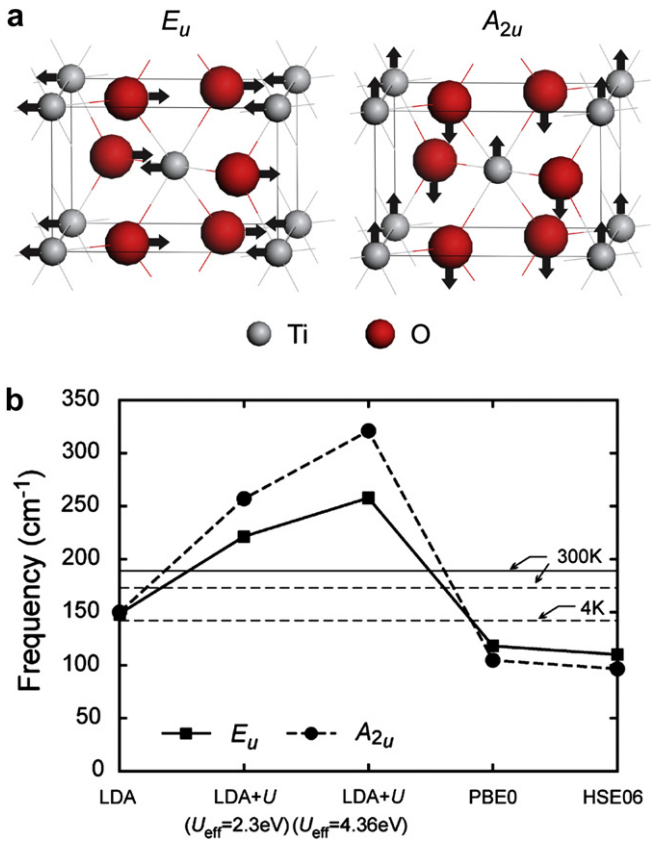

Fig. 1. (a) Lowest phonon modes in rutile TiO_2. (b) Frequencies of phonon modes in (a) computed with different energy functionals.

In the above, the LDA + U method severely underestimated dielectric constants of rutile TiO_2. A remaining question is whether the method causes a similar problem in other materials. To investigate this, we calculate ε^0 of cubic $SrTiO_3$, anatase TiO_2, and ZnO using LDA and LDA + U methods. The U_{eff} values are set to 2.3 eV for $SrTiO_3$ and anatase TiO_2, and 4.7 eV for ZnO [25]. The results are summarized in Table 4. For comparison, HSE06 results are also presented. Since $SrTiO_3$ shows ferroelectric instability within HSE06 scheme [24], the lattice parameter is adjusted to the LDA value. It is found that ε^0 of $SrTiO_3$ is significantly underestimated within the LDA + U method, similarly to rutile TiO_2. Consistently, the analysis on the phonon spectrum of $SrTiO_3$ indicates that the frequency of the TO_1 mode in LDA + U results increases to 120 cm^{-1} from the LDA value of 60 cm^{-1}. Experimentally, the mode is assigned at 40–90 cm^{-1} [24]. The dielectric constants of anatase TiO_2 is also underestimated but to a much lesser degree. On the other hand, the computed dielectric constants of ZnO agree well with experiment regardless of the employed functional. This may hint that only high-dielectric constant materials are affected significantly by the LDA + U method.

The LDA + U method has been popular in the first-principles study of $SrTiO_3$ and its heterostructures. This is mainly because the correlation effects in Ti atoms with finite d-occupancy are properly addressed within the LDA + U framework, as demonstrated in the example of $LaTiO_3$ [5]. In Refs. [5] and [9], the heterostructures of

Table 4
Static dielectric constants of $SrTiO_3$ (cubic), TiO_2 (anatase), and ZnO (wurzite), calculated with LDA and LDA + U methods. In calculating dielectric constants of $SrTiO_3$ with the HSE06 functional, the lattice parameter is fixed to those of LDA values.

	$SrTiO_3$ (cubic)	TiO_2 (anatase)		ZnO (wurzite)	
	E	ε_a	ε_c	ε_a	ε_c
LDA	662.9	53.0	27.2	8.8	9.5
LDA+U	93.0	34.9	22.1	7.8	8.6
HSE06	181.8	56.2	26.3	7.7 [29]	8.4 [29]
Expt.	301 [24]	45.1 [28]	22.7 [28]	7.8 [29]	8.9 [29]

Table 5
The effect of semicore states in TiO_2. In SC, $3s^2 3p^6$ levels are treated as valence while NC indicates that these levels are frozen as core levels. U_{eff} of 2.3 eV is used for the LDA + U method.

	LDA		LDA + U		HSE06	
	SC	NC	SC	NC	SC	NC
a (Å)	4.558	4.571	4.575	4.589	4.588	4.612
c (Å)	2.926	2.927	2.953	2.964	2.951	2.953
E_g (eV)	1.81	1.67	2.06	1.92	3.39	3.13
ε_a	149.6	107.0	58.9	46.0	277.5	141.3
ε_c	230.6	146.4	73.3	55.9	401.7	182.5

$LaTiO_3/SrTiO_3$ were studied within LDA + U methods, and it was found that the ferroelectric-like lattice relaxation in $SrTiO_3$ screens the electrostatic potential of the charged layer and significantly affects the carrier distribution in $SrTiO_3$. According to the present analysis, the hardening of $SrTiO_3$ phonon modes may suppress the dielectric screening of the charged layer and result in a narrow carrier distribution in $SrTiO_3$. Indeed, the charge profiles in Refs. [5] and [9] were sharper than the experimental observation [26]. Similarly, the charge distribution in $LaAlO_3/SrTiO_3$ heterostructures could be influenced by the same problem[10].

Lastly, we study on the effect of semicore electrons in Ti atoms. It is known that the inclusion of semicore $3s^2 3p^6$ levels of Ti into the valence improves transferability and can achieve accuracy at the level of all-electron calculations. However, it also increases the computational cost significantly and often the semicore levels are frozen as core states in large-scale calculations. In Table 5, we compare the effect of valence configurations in the Ti atom on the computed ε^0. We recall that all calculations up to this point have been carried out with semicore electrons treated as valence states. From the table, it is found that freezing the semicore states has an effect of lowering dielectric constants throughout all methods. This is contrasted to the increased lattice parameters. It is seen that HSE06 results are in the best agreement with experiment when the semicore states are frozen.

4. Summary

In summary, we investigated the dielectric properties of rutile TiO_2 using various energy functional such as LDA, LDA + U, and hybrid functional methods (PBE0 and HSE06). The computed dielectric constants significantly vary over the employed method, which was attributed to different frequencies in soft phonon modes. The LDA methods resulted in the best agreement with experiment, while the hybrid functional and LDA + U method overestimated and underestimated the dielectric constants, respectively. In particular, the underestimation by the LDA + U method was most serious. While the overestimation in the hybrid method can be corrected by using LDA lattice parameters, the problem persists with the LDA + U method. Furthermore, the LDA + U method also underestimates ε^0 of cubic $SrTiO_3$. The present results suggest that one needs to be careful in studying high-dielectric constant materials using the LDA + U method.

Acknowledgements

This study was supported by the IT R&D program of MKE/IITA, “Capacitor technology for next generation DRAMs having mass-production compatibility” (2009-F-013-01). The authors would like to acknowledge the support from the KISTI Supercomputing Center (KSC-2009-S03-0008).

References

[1] S.K. Kim, G.-J. Choi, S.Y. Lee, M. Seo, S.W. Lee, J.H. Han, H.-S. Ahn, S. Han, C.S. Hwang, Adv. Mater. 20 (2008) 1429.
[2] R.A. Parker, Phys. Rev. 124 (1961) 1719.
[3] C. Lee, P. Chose, X. Gonze, Phys. Rev. B. 50 (1994) 13379.
[4] B. Montanari, N.M. Harrison, Chem. Phys. Lett. 364 (2002) 528.
[5] H.-S. Ahn, D.D. Cuong, J. Lee, S. Han, J. Kor. Phys. Soc. 49 (2006) 1536.
[6] C. Mattioli, F. Filippone, P. Alippi, A.A. Bonapasta, Phys. Rev. B. 78 (2008) 241201 (R).
[7] A. Janotti, J.B. Varley, P. Rinke, N. Umezawa, G. Kresse, C.G. Van de Walle, Phys. Rev. B. 81 (2010) 085212.
[8] D.D. Cuong, B. Lee, K.M. Choi, H.-S. Ahn, S. Han, J. Lee, Phys. Rev. Lett. 98 (2007) 115503.
[9] S. Okamoto, A.J. Millis, N.A. Spaldin, Phys. Rev. Lett. 97 (2006) 056802.
[10] R. Pentcheva, W.E. Picket, Phys. Rev. B. 78 (2008) 205106.
[11] G. Kresse, J. Furthmüller, Phys. Rev. B. 54 (1996) 11169.
[12] J. Perdew, A. Zunger, Phys. Rev. B. 23 (1981) 5048.
[13] J. Perdew, K. Burke, M. Ernzerhof, Phys. Rev. Lett. 77 (1996) 3865.
[14] S.L. Dudarev, G.A. Botton, S.Y. Savrasov, C.J. Humphreys, A.P. Sutton, Phys. Rev. B. 57 (1998) 1505.
[15] C. Adamo, V. Barone, J. Chem. Phys. 110 (1999) 6158.
[16] A.V. Krukau, O.A. Vydrov, A.F. Izmaylov, G.E. Scuseriaa, J. Chem. Phys. 125 (2006) 224106.
[17] P. Blöchl, Phys. Rev. B. 50 (1994) 17953.
[18] X. Gonze, C. Lee, Phys. Rev. B. 55 (1997) 10355.
[19] S. Park, B. Lee, S.H. Jeon, S. Han, Curr. Appl. Phys. (2010), doi:10.1016/j.cap.2010.09.008.
[20] K. Vos, J. Phys. C: Solid State Phys. 10 (1977) 3917.
[21] F. Labat, P. Baranek, C. Domain, C. Minot, C. Adamo, J. Chem. Phys. 126 (2007) 154703.
[22] J.G. Traylor, H.G. Smith, R.M. Nicklow, M.K. Wilkinson, Phys. Rev. B. 3 (1971) 3457.
[23] G.A. Samara, P.S. Peercy, Phys. Rev. B. 7 (1973) 1131.
[24] R. Wahl, D. Vogtenhuber, G. Kresse, Phys. Rev. B. 78 (2008) 104116.
[25] A. Janotti, C.G. Van de Walle, Phys. Rev. B. 76 (2007) 165202.
[26] A. Ohtomo, D.A. Muller, J.L. Grazul, H.Y. Hwang, Nature 419 (2002) 378.
[27] J.K. Burdett, T. Hughbanks, G.J. Miller, J.W. Richardson Jr., J.V. Smith, J. Am. Chem. Soc. 109 (1987) 3639.
[28] R.J. Gonzalez, R. Zallen, H. Berger, Phys. Rev. B. 55 (1997) 7014.
[29] J. Wróbel, K.J. Kurzydłowski, K. Hummer, G. Kresse, J. Piechota, Phys. Rev. B. 80 (2009) 155124.